bioRxiv preprint doi: https://doi.org/10.1101/018846; this version posted May 1, 2015. The copyright holder for this preprint (which was not certified by peer review) is the author/funder. All rights reserved. No reuse allowed without permission.

A novel SOD1-dependent mechanism for the iron-induced production of toxic SOD1 and oxidative stress that initiates ALS

Liangzhong Lim and Jianxing Song*

Department of Biological Sciences, Faculty of Science, National University of Singapore, Republic of Singapore

Short title: Iron interferes in hSOD1 maturation

*Correspondence should be addressed to Jianxing Song, phone; 65 65161013; email: dbssjx@nus.edu.sg

The authors declare no conflict of interest.

bioRxiv preprint doi: https://doi.org/10.1101/018846; this version posted May 1, 2015. The copyright holder for this preprint (which was not certified by peer review) is the author/funder. All rights reserved. No reuse allowed without permission.

Abstract

Free iron is highly toxic and the blood-derived iron initiates early motor-neuron degeneration upon breakdown of blood-spinal cord barrier. Iron is currently known to trigger oxidative stress by Fenton chemistry but no report implies that iron manifests its toxicity through CuZn-superoxide dismutase (SOD1), the central antioxidant enzyme in all human tissues and carries >180 ALS-causing mutations. Here, by NMR we show that Zn^{2+} play an irreplaceable role in the maturation of the nascent hSOD1, and decipher for the first time that Fe^{2+} has the Zn^{2+}-like capacity in triggering the folding to form the Fe^{2+}-bound hSOD1. This acts to reduce or even block the maturation of wild-type and ALS-causing mutant hSOD1, consequently provoking oxidative stress and trapping SOD1 in toxic forms. Our study thus establishes a novel SOD1-dependent mechanism for iron to manifest its cellular toxicity which contributes to pathogenesis of neurodegenerative diseases, aging or even more.

Key words: Amyotrophic lateral sclerosis (ALS); Superoxide dismutases 1 (SOD1); Iron; Zinc; protein folding; NMR spectroscopy.

bioRxiv preprint doi: https://doi.org/10.1101/018846; this version posted May 1, 2015. The copyright holder for this preprint (which was not certified by peer review) is the author/funder. All rights reserved. No reuse allowed without permission.

Amyotrophic lateral sclerosis (ALS) is the most prominent adult motor-neuron disease, clinically characteristic of progressive motor-neuron loss in the spinal cord, brainstem, and motor cortex, which leads to paralysis and death within a few years of disease onset. ALS was first described in 1869, which affects approximately 1-2 per 100,000 people worldwide (1-3). Most ALS cases are sporadic (90%) whereas 10% are familial ALS. Accumulation of iron within CNS was recently identified to be a biomarker of ALS (4-6). Very recently, it has been revealed that in the $SOD1^{G93A}$ mice, the breakdown of blood–spinal cord barrier (BSCB) in the early ALS disease phase led to accumulation of blood-derived iron in the spinal cord, which initiates ALS by triggering early motor-neuron degeneration through iron-induced oxidant stress (7).

Higher eukaryotic aerobic organisms including humans cannot exist without oxygen, but oxygen is inherently dangerous to their existence because of oxidative stress (8-11). Oxidative stress is caused by reactive oxygen species (ROS) arising as by-products of aerobic metabolism, by which superoxide radical is formed in the greatest amount in the metabolism of molecular oxygen. The cell combats harmful ROS with multi-faceted anti-oxidant mechanisms, including catalytic removal of reactive species by enzymes such as superoxide dismutases (SOD), which removes superoxide radicals by catalyzing a dismutation reaction where one superoxide radical is oxidized to form dioxygen and another is reduced to hydrogen peroxide (12-14). Whilst superoxide and hydrogen peroxide are not highly reactive, they can further react to form highly reactive oxidants, such as hydroxyl radical ($^{\cdot}OH$), which are extremely reactive and can cause various damages to proteins, lipids and DNA, thus leading to cell death (8-14). These reactions can be radically accelerated in the presence of reduced metal ions, such as ferrous (8,9).

bioRxiv preprint doi: https://doi.org/10.1101/018846; this version posted May 1, 2015. The copyright holder for this preprint (which was not certified by peer review) is the author/funder. All rights reserved. No reuse allowed without permission.

Three superoxide dismutase isoenzymes are present within human cells, out of which CuZn-superoxide dismutase (hSOD1) is ubiquitously expressed in all tissues and primarily localized in the cytosol, the intermembrane space of mitochondria and the nucleus. hSOD1 is the most abundant, comprising ~1% of total protein in neurons (12-14). In 1993, hSOD1 was identified to be the first gene associated with FALS (15), and mutations in the SOD1 gene cause the most prevalent form of FALS, accounting for ~20% of total FALS cases (14-16). Currently, 181 mutations have been identified within the 153-residue hSOD1 that are linked to ALS (http://alsod.iop.kcl.ac.uk/) but their mechanism for triggering ALS pathogenesis remains elusive (16).

Previous studies have established that the mature hSOD1 is a homodimeric enzyme of remarkably high stability, with each subunit folding into an eight-stranded, Greek-key β-barrel, which is stabilized by an intramolecular disulfide bridge Cys57-Cys146 (12-14). Each subunit holds one copper and one zinc ions in close proximity. While Zn^{2+} is coordinated by His63, His71, His80, and Asp83, while Cu^{+} is ligated by His46, His48, and His120 (12-14) (Figure 1B). However, for the nascent hSOD1 monomer to reach the mature state, a complex multi-step maturation is required in which the critical first step is to recruit zinc, followed by the incorporation of copper and formation of the disulfide bridge catalyzed by copper chaperone for SOD1 (CCS). In contrast to the mature hSOD1, its early species particularly those lacking of the disulfide bridge have been widely shown to have high tendency of aggregation (12-15,17-21). To minimize aggregation, the mutated hSOD1 including the super-stable C6A/C111S mutant were extensively used such as for determining NMR structures lacking of the disulfide bridge (18). Nevertheless, recently it has been found that hSOD1 of the native sequence was highly disordered before metalation and formation of the disulfide bridge *in vivo* (19,20) as well as *in vitro* (21). Even upon excess supplement of zinc,

bioRxiv preprint doi: https://doi.org/10.1101/018846; this version posted May 1, 2015. The copyright holder for this preprint (which was not certified by peer review) is the author/funder. All rights reserved. No reuse allowed without permission.

only a population of the unfolded ensemble (Figure 1A) becomes well-folded (Figure 1B), which results in establishment of equilibrium between two forms (19-21).

So far, only zinc is known to own the capacity to trigger the establishment of equilibrium between the unfolded and folded hSOD1. In the present study, by high-resolution NMR characterization, we decode for the first time that Fe^{2+} has the Zn^{2+}-like capacity to induce folding to form well-folded Fe^{2+}-bound hSOD1. This decodes that Fe^{2+} is able to manifest its cellular toxicity through a SOD1-dependent mechanism.

bioRxiv preprint doi: https://doi.org/10.1101/018846; this version posted May 1, 2015. The copyright holder for this preprint (which was not certified by peer review) is the author/funder. All rights reserved. No reuse allowed without permission.

Results

Here consistent with recent *in vivo* (19,20) and *in vitro* results (21), we found that hSOD1 of the native sequence is unfolded without metalation and disulfide bridge, as clearly reflected by its poorly-dispersed HSQC spectrum (Figure 1C), which thus mimics the nascent hSOD1. By analyzing a large set of three-dimensional NMR spectra, we succeeded in achieving its NMR assignments and Figure 1D presents its (ΔCα–ΔCβ) chemical shift, which is an indicator of the residual secondary structures in disordered proteins (21,22). The small (ΔCα–ΔCβ) chemical shifts for most residues clearly indicate that the nascent hSOD1 is an ensemble of highly disordered conformations in solution, which retains no native β-sheet structure. Furthermore, hNOEs, a sensitive indicator of the backbone motions on the ns–ps time scale (21,22), are small for all residues with an average value of −0.10 (Figure 2A). In particular, more than half of the residues have negative hNOEs, clearly indicating that this unfolded ensemble is very flexible with highly unrestricted ns–ps backbone motions. We also collected ^{15}N backbone CPMG relaxation dispersion data and found no significant dispersion, indicating that under this condition, the highly-disordered hSOD1 ensemble is lacking of significant exchanges on the μs–ms time scale with significant chemical shift differences (23).

By contrast, once Zn^{2+} was added, a well-folded population was formed as indicated by the manifestation of up-field 1D peaks (Figure 1E), as well as many well-dispersed HSQC peaks (Figure 1F), which are characteristic of the folded population. A stepwise addition of Zn^{2+} triggers gradual increases of the folded population which is largely saturated at a ratio of ~1:18 (hSOD1:zinc). Interestingly, even with the ratio reaching 1:40, the unfolded and folded conformations remain coexisting, as clearly reflected by the presence of two HSQC peaks (one characteristic of unfolded and another of unfolded) from the aromatic ring of Trp32 (Figure 1F). This implies that the excess presence of zinc is insufficient to completely shift the unfolded ensemble to the folded form, consistent with recent *in vivo* (19-20) and *in vitro*

bioRxiv preprint doi: https://doi.org/10.1101/018846; this version posted May 1, 2015. The copyright holder for this preprint (which was not certified by peer review) is the author/funder. All rights reserved. No reuse allowed without permission.

(17,21) observations. Amazingly, we also observed this phenomenon on the N-terminus of another ALS-causing protein TDP-43, which encodes equilibrium of the folded and unfolded ubiquitin-like domain (24).

By analyzing triple-resonance NMR spectra acquired on a double-labeled sample in the presence of Zn^{2+} at 500 μM, we have achieved sequential assignments of the folded form of the Zn^{2+}-bound hSOD1, and its (ΔCα–ΔCβ) chemical shifts were shown in Figure 1D. The very large (ΔCα–ΔCβ) chemical shifts for most residues clearly reveal that Zn^{2+} indeed has the unique capacity in triggering the formation of the well-folded structure, consistent with recent in-cell results (19,20). Previously, a Zn^{2+}-bound structure of hSOD1 with super-stable mutations (C6A/C11S) was determined by NMR (18), and Figure 2B presents (ΔCα–ΔCβ) chemical shifts of this super-stable mutant (BMRB Entry 6821) and our folded hSOD1 of the native sequence. The results showed that except for several residues close to the mutation site C6 and C111, the (ΔCα–ΔCβ) chemical shifts of both forms are highly similar for the assigned residues. This provides strong evidence that upon binding to Zn^{2+}, both of them adopt highly similar structures despite having difference of two residues.

The well-dispersed peaks disappeared upon adding EDTA at an equal molar concentration of Zn^{2+} (Figure 1F), confirming that the formation of the folded species is a Zn^{2+}-specific effect. This highlights the irreplaceable role of Zn^{2+} in initiating the hSOD1 maturation process (17,19,20). Indeed, previous folding studies have deciphered that zinc modulates the entire folding free energy surface of hSOD1 (26).

The most unexpected finding in this study is that except for Zn^{2+}, Fe^{2+} owns the capacity in triggering the folding to form the well-folded Fe^{2+}-bound hSOD1. As seen in Figure 3A, addition of Fe^{2+} triggers the manifestation of up-field NMR peaks characteristic of the folded form and the increase in the folded population is mostly saturated at a molar ratio of 1:20 (hSOD1: Fe^{2+}). However, a detailed comparison of the intensity of up-field peaks

bioRxiv preprint doi: https://doi.org/10.1101/018846; this version posted May 1, 2015. The copyright holder for this preprint (which was not certified by peer review) is the author/funder. All rights reserved. No reuse allowed without permission.

induced by Fe^{2+} to that by Zn^{2+} is impossible as Fe^{2+} has strong paramagnetic effects including effects of relaxation enhancement and pseudo-contact shift (27). Figure 3B presents the superimposition of the HSQC spectra of the Fe^{2+}- and Zn^{2+}-bound hSOD1 forms respectively. many peaks from the Fe^{2+}-bound hSOD1 are highly superimposable to those of the Zn^{2+}-bound; while some have significant shifts. Moreover, the up-filed and well-dispersed HSQC peaks also disappeared upon adding EDTA at an equal molar concentration of Fe^{2+}, confirming that the formation of the folded hSOD1 is also Fe^{2+}-specific effect.

bioRxiv preprint doi: https://doi.org/10.1101/018846; this version posted May 1, 2015. The copyright holder for this preprint (which was not certified by peer review) is the author/funder. All rights reserved. No reuse allowed without permission.

Discussion

Oxidative stress, resulting from an imbalance between the production of free radicals and the ability of the cell to remove them, has been increasingly identified to cause various human diseases, particularly neurodegenerative diseases (7-11). In this context, hSOD1 represents a central antioxidant while iron acts as a notorious accelerator. Iron is a double-edged sword: it is the most abundant "trace element" absolutely required for humans' survival, but high levels of iron quickly lead to cell death. Under the normal conditions, the cellular concentration of free iron is very low (22,28), but under the pathological conditions such as the breakdown of the blood-central nerve system characteristic of neurodegenerative diseases and aging (29,30), the concentration of the blood-derived iron can reach very high (4-7). Indeed, iron is accumulated in various neurodegenerative as well as other diseases but the underlying mechanisms for its toxicity still remain to be fully elucidated (31-36). Currently, iron is known to trigger oxidative stress mainly through its reactivity with peroxide, thus generating the highly reactive hydroxyl radical by Fenton chemistry (8, 31-36). So far, there is no report implying that iron might manifest its cellular toxicity by specifically targeting hSOD1.

Here, by high-resolution NMR studies, we first demonstrated that the hSOD1 of the native sequence is highly disordered, and Zn^{2+} plays an irreplaceable role in initiating its maturation by triggering the formation of the folded population bound to Zn^{2+}. Previous studies revealed that both overall folded structure and local conformations/dynamics of hSOD1 maintained by Zn^{2+} are essential for further load of copper and oxidation to form the disulfide bridge Cys57-Cys146 as catalyzed by hCCS (17,19,20). Most strikingly, in this study, for the first time, we decode that Fe^{2+} has the Zn^{2+}-like capacity to induce the folding to form the Fe^{2+}-bound hSOD1, which is most likely unable to complete further load of copper and formation of the disulfide bridge, probably partly due to the differences of the

bioRxiv preprint doi: https://doi.org/10.1101/018846; this version posted May 1, 2015. The copyright holder for this preprint (which was not certified by peer review) is the author/funder. All rights reserved. No reuse allowed without permission.

Fe^{2+}- and Zn^{2+}-bound hSOD forms in local conformations/dynamics, or/and to the fact that Fe^{2+} has the binding site partly overlapped with that of copper. Therefore, the presence of Fe^{2+} at high concentrations reduces the efficiency of the Zn^{2+}-induced maturation of both wild-type and ALS-causing mutant hSOD1. Recently the failure or even reduced efficiency of the maturation has been proposed as a common mechanism for trapping the ALS-causing mutants in the highly-toxic species without the disulfide bridge, which are also prone to aggregation (13,14). Consequently, our finding establishes a SOD1-dependent mechanism for the iron-induced production of oxidative stress, as well as highly toxic forms of the mutant and wild-type hSOD1.

In the context of numerous previous results, we propose here a mechanism by which Fe^{2+} targets hSOD1 to provoke oxidative stress as well as to create toxic hSOD1 forms (Figure 4). More specifically, the hSOD1 of the native sequence before metalation and disulfide bridge formation exists as a disordered ensemble, thus mimicking the nascent hSOD1 (Figure 4A). Upon supplement of Zn^{2+}, a conformational equilibrium is established in which the folded population is formed (Figure 4B), which is ready for further interacting with copper chaperone for hSOD1 (hCCS) (Figure 4C). This interaction leads to the formation of the mature and active hSOD1 with copper loaded and the disulfide bridge formed, which becomes a central antioxidant enzyme catalyzing the dismutation reaction (Figure 4E). However, if in the presence of Fe^{2+} at high concentrations, a population of Fe^{2+}-bound hSOD1 is forms, which has an overall architecture similar to the Zn^{2+}-bound (Figures 4F and 4G), but most likely unsuitable for further load of copper and formation of the disulfide bridge catalyzed by hCCS, As a consequence, the Fe^{2+}-bound hSOD1 form without stabilization by the disulfide bridge acquires high toxicity as found with other ALS-causing mutants including G93A and H46R/H48Q, by such as interacting with membranes of

bioRxiv preprint doi: https://doi.org/10.1101/018846; this version posted May 1, 2015. The copyright holder for this preprint (which was not certified by peer review) is the author/funder. All rights reserved. No reuse allowed without permission.

organelles (21,37) or/and become aggregated to form the iron-containing hSOD1 inclusion (Figure 4H) extensively observed in ALS patients.

Our study also raises some interesting issues to be explored in the future. For example, it remains to investigate whether the Fe^{2+}-bound hSOD1, which is chemically similar to Cu^{+}-bound hSOD1, also acquires the activity to catalyze endogenous production of nitric oxide to induce apoptosis, as previously detected on the copper-bound, zinc-deficient SOD1 (38). Nevertheless, the high-resolution NMR results unequivocally decipher that in addition to Fenton reaction (Figure 4I), Fe^{2+} is also able to manifest its toxicity through a SOD1-dependent mechanism, by which Fe^{2+} is able to trap the mutant or even wild-type hSOD1 into highly toxic forms; as well as to provoke significant oxidative stress (Figure 4J). Both are expected to contribute to pathogenesis of neurodegenerative diseases including ALS as well as aging. This may partly rationalize the observation that under certain pathological conditions, the wild-type hSOD1 is also able acquire toxicity to initiate ALS. Furthermore, as hSOD1 exists in all human tissues, the hSOD1-dependent mechanism we decipher here is expected also to play general roles in triggering other diseases upon the bio-availability of Fe^{2+} at high concentrations. Our study also provides mechanistic supports to the therapeutic approaches to treat neurodegenerative diseases or to slow down aging by repairing the breakdown of the blood-central nerve system barrier and intaking iron-chelators by design or/and from natural products such as in fruits and green tea (32-40).

bioRxiv preprint doi: https://doi.org/10.1101/018846; this version posted May 1, 2015. The copyright holder for this preprint (which was not certified by peer review) is the author/funder. All rights reserved. No reuse allowed without permission.

Methods

Preparation of the wild-type and mutant hSOD1proteins.

The gene encoding hSOD1 was purchased from Genscript with *E. coli* preferred codons (21). The overexpressed was conducted in *Escherichia coli* BL21 (DE3) cells (Novagen). The generation of the isotope-labeled proteins for NMR studies followed a similar procedure except that the bacteria were grown in M9 medium with the addition of $(^{15}NH_4)_2SO_4$ for ^{15}N labeling and $(^{15}NH_4)_2SO_4$ /[^{13}C]-glucose for ^{15}N-/^{13}C-double labelling (21). The purity of the recombinant proteins was checked by SDS–PAGE gels and verified by a Voyager STR matrix-assisted laser desorption ionization time-of-flight-mass spectrometer (Applied Biosystems), as well as NMR assignments. The concentration of protein samples was determined by the UV spectroscopic method in the presence of 8 M urea (21).

NMR experiments.

All NMR experiments were acquired at 25 degree on an 800 MHz Bruker Avance spectrometer equipped with pulse field gradient units as described previously (21,23,24). For characterizing the unfolded hSOD1 ensemble, a pair of triple-resonance experiments HNCACB, CBCA(CO)NH were collected for the sequential assignment on a ^{15}N-/^{13}C-double labelled sample of 500 μM, while ^{15}N-edited HSQC-TOCSY and HSQC-NOESY were collected on a ^{15}N-labelled sample at a protein concentration of 500 μM. For achieving assignments of the folded hSOD1 induced by Zn^{2+}, triple-resonance experiments HNCACB, CBCA(CO)NH were collected for on a ^{15}N-/^{13}C-double labelled sample of 500 μM in the presence of Zn^{2+}.

For assessing the backbone dynamics of the unfolded hSOD1 ensemble on the ps-ns time scale, $\{^1H\}$-^{15}N steady-state NOEs were obtained by recording spectra on the ^{15}N-

bioRxiv preprint doi: https://doi.org/10.1101/018846; this version posted May 1, 2015. The copyright holder for this preprint (which was not certified by peer review) is the author/funder. All rights reserved. No reuse allowed without permission.

labeled sample at 500 μM with and without ^{1}H presaturation with duration of 3 s plus a relaxation delay of 6 s at 800 MHz. To assess conformational exchanges over μs-ms, ^{15}N transverse relaxation dispersion experiments were acquired on the ^{15}N-labeled sample on a Bruker Avance 800 spectrometer with a constant time delay (TCP = 50 ms) and a series of CPMG frequencies, ranging from 40 Hz, 80 Hz, 120 Hz (x3), 160 Hz, 200 Hz, 240 Hz, 320 Hz, 400 Hz, 480 Hz, 560 Hz, 640 Hz, 720 Hz, 800 Hz, and 960 Hz (×3 indicates repetition) as we previously performed (21,23).

bioRxiv preprint doi: https://doi.org/10.1101/018846; this version posted May 1, 2015. The copyright holder for this preprint (which was not certified by peer review) is the author/funder. All rights reserved. No reuse allowed without permission.

References

1. Bruijn LI, Miller TM, Cleveland DW (2004) Unraveling the mechanisms involved in motor neuron degeneration in ALS. *Annu. Rev. Neurosci*. 27: 723–749.

2. Kiernan MC, et al. (2011) Amyotrophic lateral sclerosis. Lancet 377(9769):942–955.

3. Zlokovic BV (2011) Neurovascular pathways to neurodegeneration in Alzheimer's disease and other disorders. Nat Rev Neurosci 12(12):723–738.

4. Oba H, et al. (1993) Amyotrophic lateral sclerosis: T2 shortening in motor cortex at MR imaging. Radiology 189(3):843–846.

5. Kwan JY, et al. (2012) Iron accumulation in deep cortical layers accounts for MRI signal abnormalities in ALS: Correlating 7 tesla MRI and pathology. PLoS ONE 7(4):e35241.

6. Ignjatović A, Stević Z, Lavrnić S, Daković M, Bačić G. Brain iron MRI: a biomarker for amyotrophic lateral sclerosis. J Magn Reson Imaging. 2013 Dec;38(6):1472-9. doi: 10.1002/jmri.24121.

7. Winkler EA, Sengillo JD, Sagare AP, Zhao Z, Ma Q, Zuniga E, Wang Y, Zhong Z, Sullivan JS, Griffin JH, Cleveland DW, Zlokovic BV. Blood-spinal cord barrier disruption contributes to early motor-neuron degeneration in ALS-model mice. Proc Natl Acad Sci U S A. 2014 Mar 18;111(11):E1035-42. doi: 10.1073/pnas.1401595111

8. B. Halliwell, J.M.C. Gutteridge, Free Radicals in Biology and Medicine, 3rd ed., Oxford Univ. Press, Oxford, 1999.

9. Simonian NA, Coyle JT. Oxidative stress in neurodegenerative diseases. Annu Rev Pharmacol Toxicol. 1996;36:83-106.

10. Markesbery, W.R. Oxidative stress hypothesis in Alzheimer's disease. Free Radic. Bioi. Med. 1997, 23(1), 134-147.

bioRxiv preprint doi: https://doi.org/10.1101/018846; this version posted May 1, 2015. The copyright holder for this preprint (which was not certified by peer review) is the author/funder. All rights reserved. No reuse allowed without permission.

11. Barber SC, Mead RJ, Shaw PJ. Oxidative stress in ALS: a mechanism of neurodegeneration and a therapeutic target. Biochim Biophys Acta. 2006 Nov-Dec;1762(11-12):1051-67.

12. Fridovich I. Superoxide dismutases. Annu Rev Biochem. 1975;44:147-59.

13. Sheng Y, Abreu IA, Cabelli DE, Maroney MJ, Miller AF, Teixeira M, Valentine JS. Superoxide dismutases and superoxide reductases. Chem Rev. 2014 Apr 9;114(7):3854-918. doi: 10.1021/cr4005296.

14. Valentine JS, Doucette PA, Zittin Potter S. Copper-zinc superoxide dismutase and amyotrophic lateral sclerosis. Annu Rev Biochem. 2005;74:563-93.

15. Rosen DR, Siddique T, Patterson D, Figlewicz DA, Sapp P, Hentati A, Donaldson D, Goto J, O'Regan JP, Deng HX, et al. Mutations in Cu/Zn superoxide dismutase gene are associated with familial amyotrophic lateral sclerosis. Nature. 1993 Mar 4;362(6415):59-62.

16. Abel O, Powell JF, Andersen PM, Al-Chalabi A ALSoD: (2012) A user-friendly online bioinformatics tool for amyotrophic lateral sclerosis genetics. *Hum Mutat.* 33(9):1345-1351.

17. Banci L1, Bertini I, Cantini F, Kozyreva T, Massagni C, Palumaa P, Rubino JT, Zovo K. Human superoxide dismutase 1 (hSOD1) maturation through interaction with human copper chaperone for SOD1 (hCCS). Proc Natl Acad Sci U S A. 2012 Aug 21;109(34):13555-60. doi: 10.1073/pnas.1207493109.

18. Banci L , Bertini I, Cantini F, D'Amelio N, Gaggelli E (2006) Human SOD1 before harboring the catalytic metal: solution structure of copper-depleted, disulfide-reduced form. *J Biol Chem.* 281(4):2333-2337.

19. Banci L, Barbieri L, Bertini I, Luchinat E, Secci E, Zhao Y, Aricescu AR. Atomic-resolution monitoring of protein maturation in live human cells by NMR. Nat Chem Biol. 2013 May;9(5):297-9. doi: 10.1038/nchembio.1202.

bioRxiv preprint doi: https://doi.org/10.1101/018846; this version posted May 1, 2015. The copyright holder for this preprint (which was not certified by peer review) is the author/funder. All rights reserved. No reuse allowed without permission.

20. Luchinat E, Barbieri L, Rubino JT, Kozyreva T, Cantini F, Banci L. In-cell NMR reveals potential precursor of toxic species from SOD1 fALS mutants. Nat Commun. 2014 Nov 27;5:5502. doi: 10.1038/ncomms6502.

21. Lim L, Lee X, Song J. Mechanism for transforming cytosolic SOD1 into integral membrane proteins of organelles by ALS-causing mutations. Biochim Biophys Acta. 2015 Jan;1848(1 Pt A):1-7. doi: 10.1016/j.bbamem.2014.10.002.

22. Dyson HJ, Wright PE (2004) Unfolded proteins and protein folding studied by NMR, *Chem. Rev.* 104(8): 3607–3622.

23. Qin H, Lim LZ, Song J. Dynamic principle for designing antagonistic/agonistic molecules for EphA4 receptor, the only known ALS modifier. ACS Chem Biol. 2015 Feb 20;10(2):372-8. doi: 10.1021/cb500413n.

24. Qin H, Lim LZ, Wei Y, Song J. TDP-43 N terminus encodes a novel ubiquitin-like fold and its unfolded form in equilibrium that can be shifted by binding to ssDNA. Proc Natl Acad Sci U S A. 2014 Dec 30;111(52):18619-24. doi: 10.1073/pnas.1413994112.

26. Kayatekin C1, Zitzewitz JA, Matthews CR. Zinc binding modulates the entire folding free energy surface of human Cu,Zn superoxide dismutase. J Mol Biol. 2008 Dec 12;384(2):540-55. doi: 10.1016/j.jmb.2008.09.045.

27. Otting G. Protein NMR using paramagnetic ions. Annu Rev Biophys. 2010;39:387-405. doi: 10.1146/annurev.biophys.093008.131321.

28. Andrews NC, Schmidt PJ. Iron homeostasis. Annu Rev Physiol. 2007;69:69-85.

29. Montagne A, Barnes SR, Sweeney MD, Halliday MR, Sagare AP, Zhao Z, Toga AW, Jacobs RE, Liu CY, Amezcua L, Harrington MG, Chui HC, Law M, Zlokovic BV. Blood-brain barrier breakdown in the aging human hippocampus. Neuron. 2015 Jan 21;85(2):296-302. doi: 10.1016/j.neuron.2014.12.032.

bioRxiv preprint doi: https://doi.org/10.1101/018846; this version posted May 1, 2015. The copyright holder for this preprint (which was not certified by peer review) is the author/funder. All rights reserved. No reuse allowed without permission.

30. Ronaldson PT1, Davis TP2. Targeting Transporters: Promoting Blood-brain barrier repair in Response to Oxidative Stress Injury. Brain Res. 2015 Mar 18. pii: S0006-8993(15)00200-0. doi: 10.1016/j.brainres.2015.03.018.

31. Rouault TA. Iron metabolism in the CNS: implications for neurodegenerative diseases. Nat Rev Neurosci. 2013 Aug;14(8):551-64. doi: 10.1038/nrn3453.

32. Ward RJ, Zucca FA, Duyn JH, Crichton RR, Zecca L. The role of iron in brain ageing and neurodegenerative disorders. Lancet Neurol. 2014 Oct;13(10):1045-60. doi: 10.1016/S1474-4422(14)70117-6.

33. Dixon SJ, Stockwell BR. The role of iron and reactive oxygen species in cell death. Nat Chem Biol. 2014 Jan;10(1):9-17. doi: 10.1038/nchembio.1416.

34. Puliyel M, Mainous AG 3rd, Berdoukas V, Coates TD. Iron toxicity and its possible association with treatment of Cancer: Lessons from hemoglobinopathies and rare, transfusion-dependent anemias. Free Radic Biol Med. 2015 Feb;79C:343-351. doi: 10.1016/j.freeradbiomed.2014.10.861.

35. Liochev SI, Fridovich I. Superoxide and iron: partners in crime. IUBMB Life. 1999 Aug;48(2):157-61.

36. Aguirre JD, Culotta VC. Battles with iron: manganese in oxidative stress protection. J Biol Chem. 2012 Apr 20;287(17):13541-8. doi: 10.1074/jbc.R111.312181.

37. Liu J, Lillo C, Jonsson PA, Vande Velde C, Ward CM, Miller TM, Subramaniam JR, Rothstein JD, Marklund S, Andersen PM, Brännström T, Gredal O, Wong PC, Williams DS, Cleveland DW. Toxicity of familial ALS-linked SOD1 mutants from selective recruitment to spinal mitochondria. Neuron. 2004 Jul 8;43(1):5-17.

38. Boillée S, Cleveland DW. Revisiting oxidative damage in ALS: microglia, Nox, and mutant SOD1. J Clin Invest. 2008 Feb;118(2):474-8. doi: 10.1172/JCI34613.

bioRxiv preprint doi: https://doi.org/10.1101/018846; this version posted May 1, 2015. The copyright holder for this preprint (which was not certified by peer review) is the author/funder. All rights reserved. No reuse allowed without permission.

Acknowledgement

We thank Ms Linlin Miao for preparing the proteins. The study is supported by Ministry of Education of Singapore (MOE) Tier 2 Grant MOE 2011-T2-1-096 (R154-000-525-112) to Jianxing Song.

bioRxiv preprint doi: https://doi.org/10.1101/018846; this version posted May 1, 2015. The copyright holder for this preprint (which was not certified by peer review) is the author/funder. All rights reserved. No reuse allowed without permission.

Figure legends

Figure 1. Zn^{2+} plays an irreplaceable role in initiating the hSOD1 maturation. Schematic representation of the unfolded ensemble (A), and mature subunit (B) of hSOD1. The folded hSOD1 is represented by the monomer of the dimeric crystal structure of the human SOD1 (1PU0). Some residues relevant to the present study are labeled. (C) Two-dimensional ^{1}H-^{15}N NMR HSQC spectrum of hSOD1 of the native sequence without metallation and disulfide bridge. (D) Residue specific (ΔCα-ΔCβ) chemical shifts of hSOD1 without metallation and disulfide bridge (blue); and of the folded form in the presence of zinc (red). (E) Up-field 1D NMR peaks characteristic of the folded SOD1 (-0.5-0.62 ppm) in the presence of zinc at different molar ratios. (F) Superimposition of HSQC spectra of hSOD1 without the disulfide bridge but in the presence of zinc at a ratio of 1:20 (SOD1:zinc) (blue) and that after addition of EDTA at an equal molar ratio of zinc. Blue arrow is used for indicating HSQC peak of the Trp32 ring proton resulting from the unfolded ensemble while red arrow for that from the folded hSOD1.

Figure 2. NMR characterization of residue-specific conformations and dynamics of the unfolded and folded hSOD1. (A) $\{^{1}H\}$-^{15}N heteronuclear steady-state NOE (hNOE) of the unfolded hSOD1 without metallation and disulfide bridge, which mimic nascent hSOD1. (B) Residue specific (ΔCα-ΔCβ) chemical shifts of the Zn^{2+}-bound hSOD1 of the native sequence (red), and those derived from the previously deposited NMR data (BMRB Entry 6821) for the Zn^{2+}-bound hSOD1 with C6A/C111S mutations (blue). The two mutation sites C6 and C111 are indicated.

bioRxiv preprint doi: https://doi.org/10.1101/018846; this version posted May 1, 2015. The copyright holder for this preprint (which was not certified by peer review) is the author/funder. All rights reserved. No reuse allowed without permission.

Figure 3. Fe^{2+} has the Zn^{2+}-like capacity in triggering the folding to form the Fe^{2+}-bound hSOD1. (A) Up-field 1D NMR peaks characteristic of the folded hSOD1 (-0.5-0.62 ppm) in the presence of Fe^{2+} at different molar ratios. (B) Superimposition of HSQC spectra of hSOD1 without the disulfide bridge but in the presence of Zn^{2+} (blue), and Fe^{2+} (red). The labels of the sequential assignments for some well-resolved HSQC peaks are in green if the peaks are largely superimposable but in pink if the peaks are largely shifted in both forms.

Figure 4. A SOD1-dependent mechanism by which Fe^{2+} provokes oxidative stress and traps the wild-type and ALS-causing mutant hSOD1 in the toxic forms.

bioRxiv preprint doi: https://doi.org/10.1101/018846; this version posted May 1, 2015. The copyright holder for this preprint (which was not certified by peer review) is the author/funder. All rights reserved. No reuse allowed without permission.

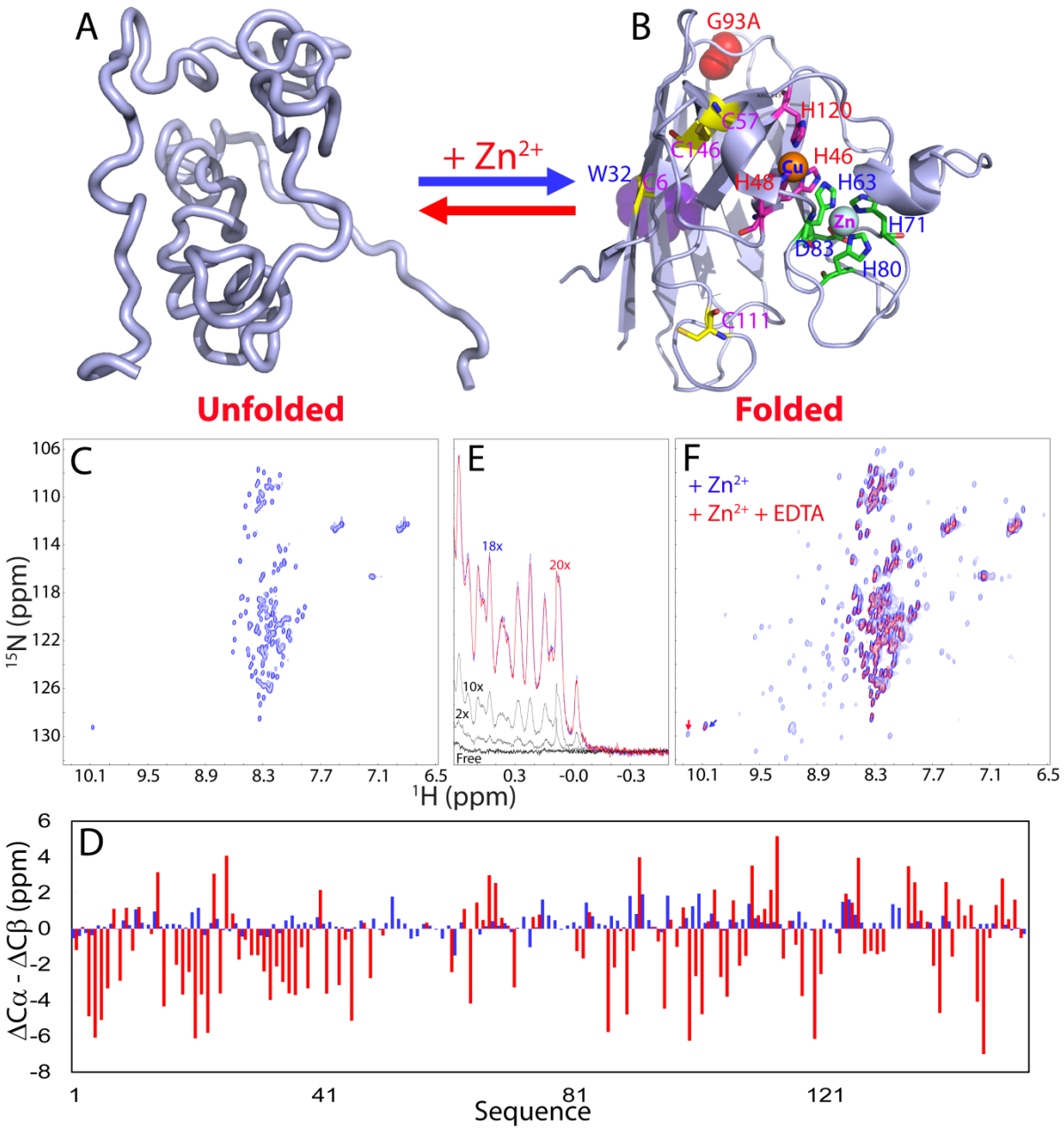

bioRxiv preprint doi: https://doi.org/10.1101/018846; this version posted May 1, 2015. The copyright holder for this preprint (which was not certified by peer review) is the author/funder. All rights reserved. No reuse allowed without permission.

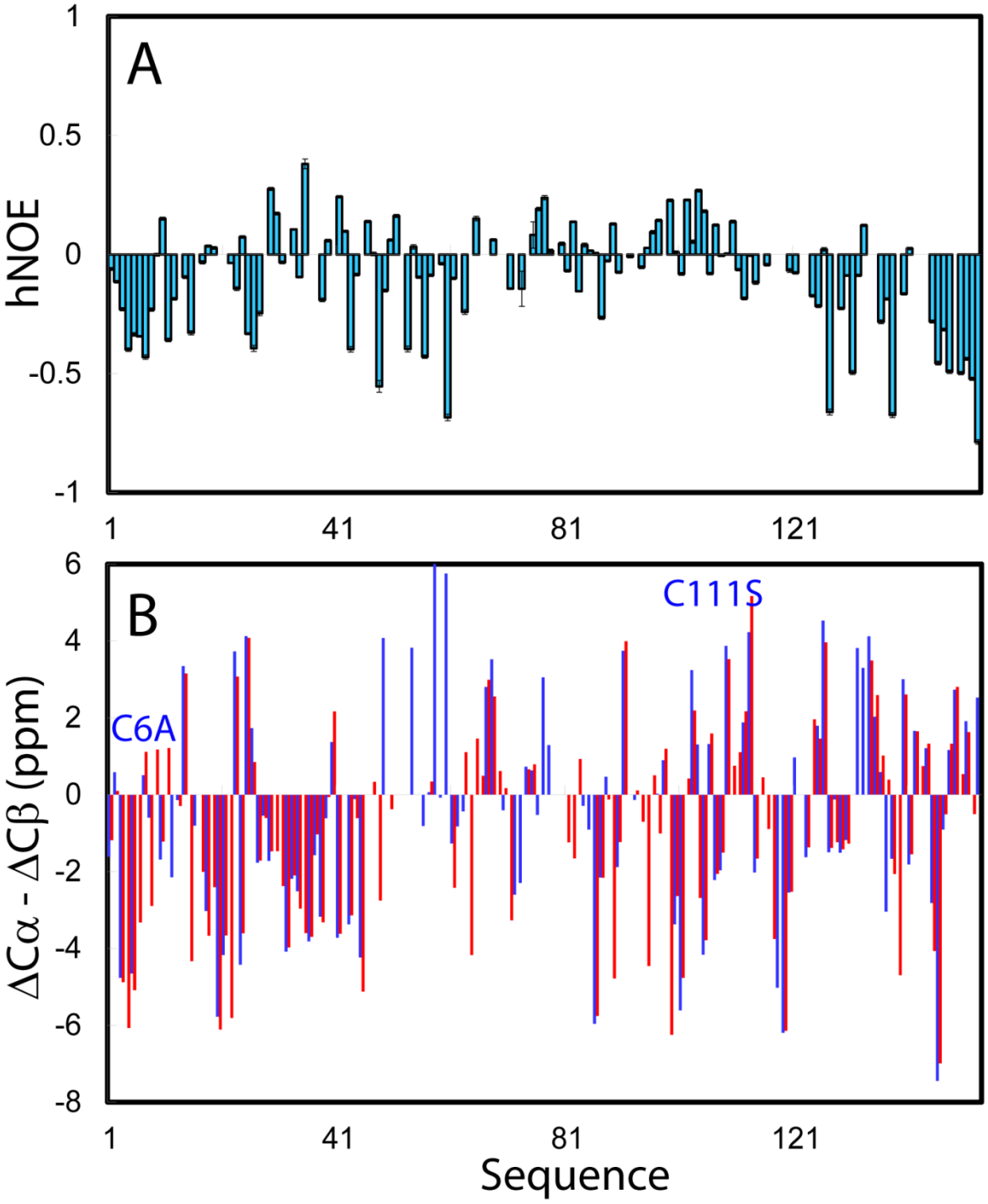

bioRxiv preprint doi: https://doi.org/10.1101/018846; this version posted May 1, 2015. The copyright holder for this preprint (which was not certified by peer review) is the author/funder. All rights reserved. No reuse allowed without permission.

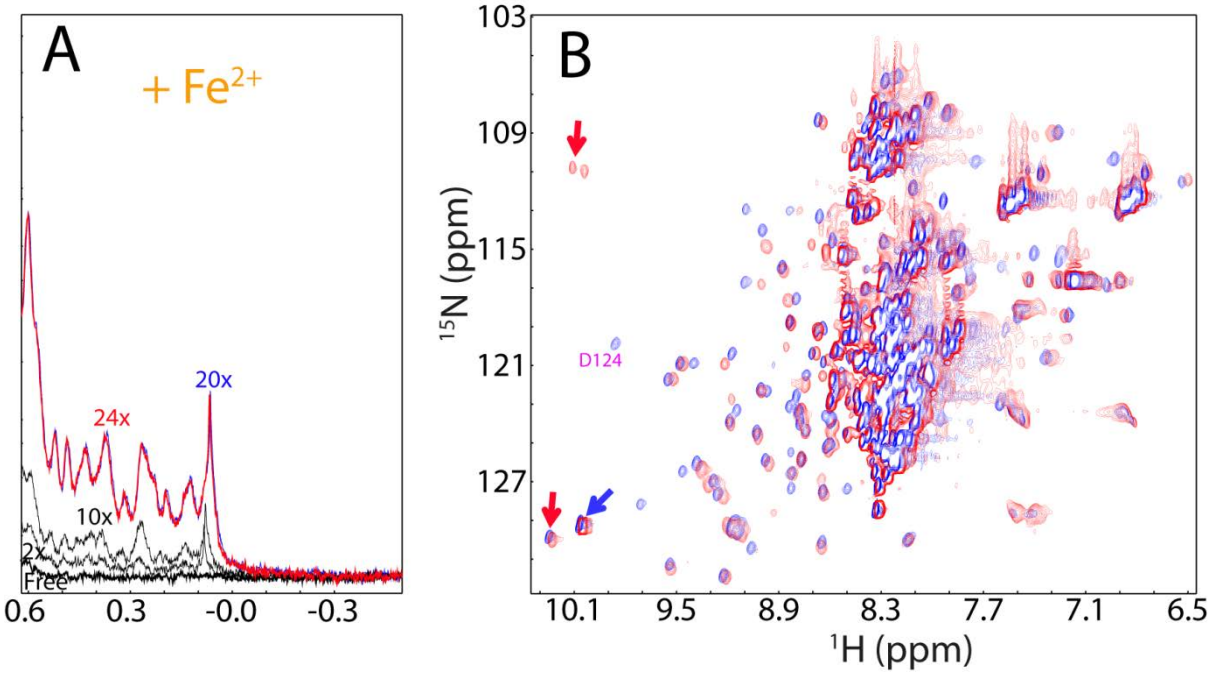
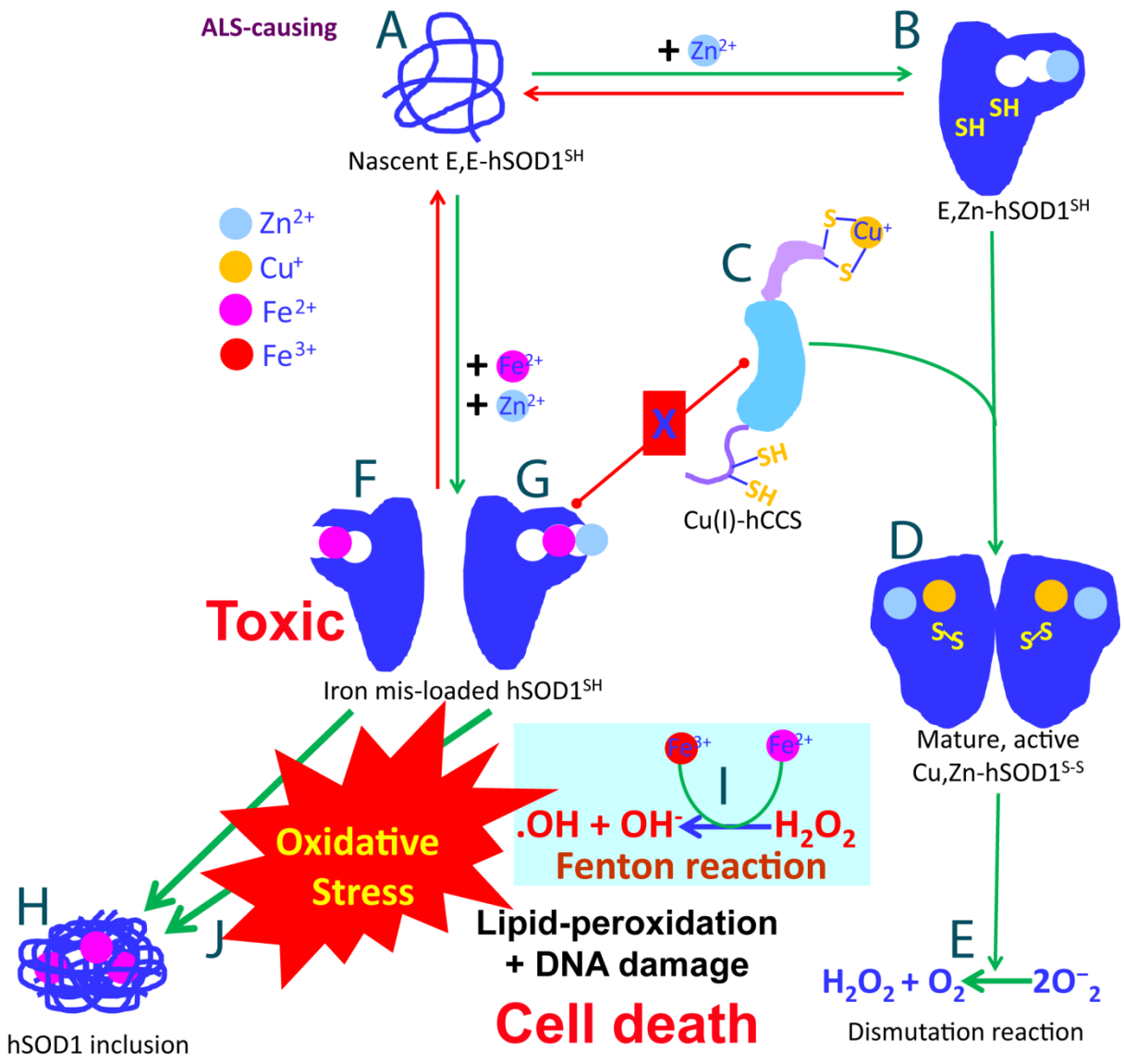
bioRxiv preprint doi: https://doi.org/10.1101/018846; this version posted May 1, 2015. The copyright holder for this preprint (which was not certified by peer review) is the author/funder. All rights reserved. No reuse allowed without permission.